


Biexciton relaxation associated with dissociation into a surface polariton pair in semiconductor filmsYasuyoshi Mitsumori,* Shimpei Matsuura, Shoichi Uchiyama, Kentarao Saito, and Keiichi Edamatsu
*Research Institute of Electrical Communication, Tohoku University, Sendai 980-8577, Japan*Masaaki Nakayama
*Department of Applied Physics, Graduate School of Engineering, Osaka City University, Osaka 558-8585, Japan*Hiroshi Ajiki
School of Science and Engineering, Tokyo Denki University, Saitama 350-0394, Japan (Received 21 November 2017; revised manuscript received 27 March 2018; published 12 April 2018)

We study the biexciton relaxation process in CuCl films ranging from 6 to 200 nm. The relaxation time is measured as the dephasing time and the lifetime. We observe a unique thickness dependence of the biexciton relaxation time and also obtain an ultrafast relaxation time with a timescale as short as 100 fs, while the exciton lifetime monotonically decreases with increasing thickness. By analyzing the exciton-photon coupling energy for a surface polariton, we theoretically calculate the biexciton relaxation time as a function of the thickness. The calculated dependence qualitatively reproduces the observed relaxation time, indicating that the biexciton dissociation into a surface polariton pair is one of the major biexciton relaxation processes.

DOI: [10.1103/PhysRevB.97.155303](https://doi.org/10.1103/PhysRevB.97.155303)**I. INTRODUCTION**

Two excitons with opposite spins in semiconductors attractively interact with each other and form a bound state, which is known as a biexciton. Biexcitons have been studied as a physical system to investigate nonlinear optical properties in solids. Earlier studies have shown giant two-photon absorption [1–3], hyperparametric scattering [4,5], and Autler-Townes splitting [6]. Recently, biexcitons have attracted attention as promising quantum light sources for quantum information technology applications, such as entangled photon pair generation using cascade radiation [7–9]. For the biexciton relaxation process, it is widely accepted that the radiative decay process emitting photons outside the crystal mainly contributes to the relaxation process in bulk, quantum well, and quantum dot systems. Various decay times of the biexciton in CuCl films and bulk crystals have been reported, ranging from a few picoseconds to several tens of picoseconds [10–15]. The reported decay time tends to be almost proportional to the thickness of the crystal. On the other hand, the exciton systems in the films show that a spatial overlap between the exciton wave function and the light wave shortens the radiative lifetime with increasing thickness [16–18], while in bulk crystals, the exciton forms polaritons, which exhibit characteristic temporal responses [19–21]. Therefore, the different thickness dependences of the biexciton and exciton lifetimes in the films suggest the presence of other key relaxation mechanisms of the biexciton. One such mechanism was pointed out in a pioneering theoretical work by Ivanov *et al.* [22], where the contribution of surface polaritons to biexciton relaxation was shown. However, systematic experimental studies of the biexciton relaxation process and

the relationship to surface polaritons as a function of crystal thickness have not yet been reported.

In this paper, we demonstrate that biexciton dissociation into a surface polariton pair plays an important role in the biexciton relaxation process by observing the dependence of the biexciton relaxation time on the thickness of CuCl films. Furthermore, we qualitatively reproduce the observed dependence theoretically by introducing the process of biexciton dissociation into a surface polariton pair into our calculations. We also observe an ultrafast relaxation time with a timescale as short as 100 fs, indicating that the biexciton relaxation is effectively enhanced by a variation in the exciton-photon composition in the dissociated surface polariton, which is strongly affected by the sample thickness. In addition, we present the experimentally obtained thickness dependence of the exciton lifetime, which monotonically decreases with increasing thickness.

II. SAMPLE AND EXPERIMENTAL METHODS

The samples used in this work were CuCl films with various thicknesses, which were grown on a (0001) Al₂O₃ substrate with a vacuum-deposition method, and each CuCl film was capped by a 270-nm-thick SiO₂ layer to prevent deliquescence of CuCl with an rf magnetron sputtering method [23]. We confirmed from x-ray diffraction patterns that the growth direction of the CuCl films was the [111] crystal axis and that the films were polycrystalline. The thicknesses of the CuCl films were $d = 6, 8, 10, 25, 50, 100, 130,$ and 200 nm, which were measured with a profilometer with a resolution of 0.5 nm.

The excitation light source was the second-harmonic light of a femtosecond mode-locked Ti:sapphire laser. The central photon energy of the incident optical pulses was tuned to 3.186 eV, which corresponds to the two-photon resonant energy of the

*mitumori@riec.tohoku.ac.jp

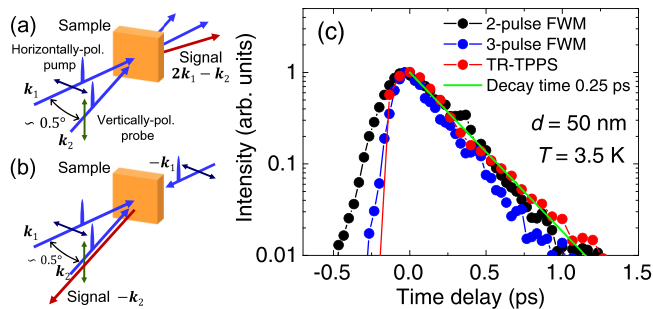


FIG. 1. Schematic diagrams of (a) the standard two-pulse FWM experiment and (b) the three-pulse phase-conjugate FWM measurement. (c) Response of the standard two-pulse and three-pulse phase-conjugate FWM intensities, together with the decay profile of the TR-TPPS signal and decay curve with a decay time constant of 0.25 ps. In all measurements, the center of the excitation laser spectrum was in two-photon resonance with the biexciton.

biexciton in a CuCl bulk crystal. The bandwidth of the pulses was set to be ~ 16 meV, and the temporal duration was ~ 100 fs. In order to obtain the biexciton relaxation time as a dephasing time T_2 , we applied a standard two-pulse four-wave-mixing (FWM) technique under the transmission geometry to all samples, as illustrated in Fig. 1(a). A horizontally polarized pump pulse with wave vector \mathbf{k}_1 creates a coherence between the biexciton B with a momentum of $2\mathbf{k}_1$ and the ground state G , i.e., ρ_{BG} in the density matrix. The vertically polarized probe pulse with \mathbf{k}_2 interacts with the coherence ρ_{BG} and induces the FWM signal along $2\mathbf{k}_1 - \mathbf{k}_2$. We detected the FWM signal intensity as a function of the time delay τ between the pump and probe pulses. In this geometry, the signal decay time constant in the positive- τ regime gives the decay time of the coherence ρ_{BG} , referred to as a two-photon dephasing time T_2^{BG} [24,25]. The angle between the pump and probe pulses was set to be as small as 0.5° , and the mean incident angle to the sample was normal to the sample surface. To investigate the propagation effect of the biexciton in the sample, we also performed a three-pulse phase-conjugate FWM measurement by introducing an additional horizontally polarized pump pulse with wave vector $-\mathbf{k}_1$, as shown in Fig. 1(b). The counterpropagating excitation created a coherence between the biexciton with zero momentum and the ground state. By observing the signal intensity emitted along $-\mathbf{k}_2$, which was induced by the probe pulse with wave vector \mathbf{k}_2 , we obtained the dephasing time of the biexciton with zero momentum, when the time delay between the two counterpropagating pump pulses was fixed at zero. The intensities of the pump and probe pulses were set to be the same, ~ 100 nJ/cm² per pulse. In order to estimate the biexciton lifetime, time-resolved two-photon polarization spectroscopy (TR-TPPS) measurements were carried out using the same experimental procedure as in Ref. [26]. We also measured a pump-induced change in the probe transmission (PP) around the exciton resonance to obtain the thickness dependence of the exciton lifetime. In this measurement, we tuned the center of the laser spectrum to the exciton resonance at 3.202 eV. The polarization configuration of the PP measurement is the same as that of the two-pulse FWM experiment. All measurements were carried out at 3.5 K.

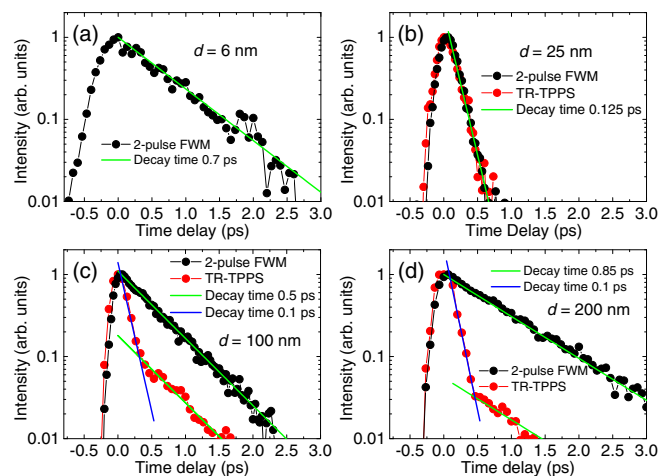


FIG. 2. FWM responses for (a) the $d = 6$ nm sample, (b) $d = 25$ nm, (c) $d = 100$ nm, and (d) $d = 200$ nm, together with fitting curves. In (b), (c), and (d), the results of the TR-TPPS measurements are shown. In all measurements, the center of the excitation laser spectrum was in two-photon resonance with the biexciton.

III. EXPERIMENTAL RESULTS

Figure 1(c) shows the results of two-pulse FWM, phase-conjugate FWM, and TR-TPPS measurements for the $d = 50$ nm sample when the center of the excitation laser spectrum is set to the two-photon resonant energy of the biexciton. The three scans showed almost the same decay time constants. From a single exponential fit, the decay time constant was estimated to be ~ 0.25 ps. The estimated FWM decay time of ~ 0.25 ps gives $T_2^{BG} \sim 0.5$ ps [27]. The signal decay time of the TR-TPPS corresponds to the decay time of the biexciton population ρ_{BB} , i.e., a biexciton lifetime T_1^B [26], and gives $T_1^B \sim 0.25$ ps. Therefore, the biexciton dephasing time around $d = 50$ nm reaches the lifetime T_1 limit, i.e., $T_2 = 2T_1$. The dephasing time depends solely on the lifetime, and the other dephasing processes, such as phonon scattering, do not contribute. The observed biexciton lifetime is much shorter than those of previous studies using bulk samples with a thickness of several tens of micrometers [10–14]. For exciton systems in CuCl thin films with a thickness less than 120 nm, an earlier study proposed that the propagation time of the exciton between the sample surfaces dominates the lifetime, referred to as the wall collision process [28]. However, the agreement with the decay time constants of the two-pulse and phase-conjugate FWM signals demonstrates that the propagation effect can be ruled out as a cause of the shorter lifetime because the phase-conjugate configuration of the pump pulses creates biexcitons with zero momentum, which do not propagate in the sample.

In Fig. 2, we present the decay profiles of the two-pulse FWM for thicknesses of $d = 6, 25, 100,$ and 200 nm, when the center of the excitation laser spectrum was set to the two-photon resonant energy of the biexciton. Except for the $d = 6$ nm sample, we plot the results of the TR-TPPS measurements. The decay time constants of the FWM and TR-TPPS signals were sensitive to the thickness. For the TR-TPPS decay profiles in the $d \geq 100$ nm samples, we observed an additional fast decay component to the signal representing the

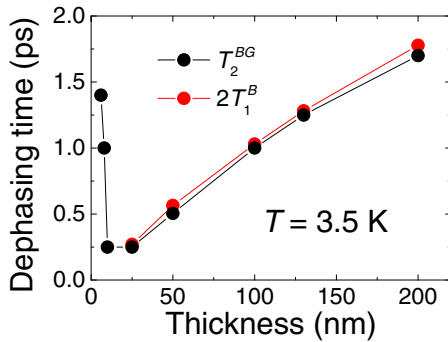


FIG. 3. Dependence of the biexciton dephasing time T_2^{BG} on the thickness. The values of $2T_1^B$ with a thickness range of 25–200 nm are plotted.

biexciton lifetime. We infer that the fast component arises from the exciton population decay because the decay time constant of the fast component of ~ 0.1 ps in the $d = 100$ nm sample agrees well with the exciton lifetime of ~ 0.12 ps, which was estimated by the PP measurement in the same sample [as shown in Fig. 4(b) below]. We give the details of the contribution of the exciton to the TR-TPPS signal later. On the other hand, for the thickness range of 6–10 nm, we could not detect the TR-TPPS signal because the TR-TPPS signal is generated by two-photon absorption [26], which becomes weaker with decreasing sample thickness. As shown in Fig. 2(b) for the $d = 25$ nm sample, we observed the shortest decay time of the FWM signal of all the samples. The decay time of ~ 0.125 ps gives the shortest dephasing time $T_2^{BG} \sim 0.25$ ps. The agreement with the decay time constants of the TR-TPPS and FWM signals indicates that the biexciton lifetime of $T_1 \sim 0.125$ ps is also the shortest and dominates the extremely fast dephasing process. We summarize the dephasing time as a function of the thickness in Fig. 3, together with the values of twice the biexciton lifetime, i.e., $2T_1^B$, with a thickness range of 25–200 nm. Figure 3 clearly shows a variation in the dephasing time dependent on the thickness. In the thickness regime $d = 6$ –10 nm, the dephasing time rapidly decreases with increasing thickness. Around $d = 10$ –25 nm, the dephasing time reaches a minimum. In the regime thicker than $d = 25$ nm, the dephasing time is almost proportional to the thickness while keeping $T_2 = 2T_1$. We infer that the biexciton lifetime in the regime thinner than $d = 10$ nm also shows the same thickness dependence as the dephasing time because the minimum dephasing time at $d = 25$ nm reaches the lifetime limit, and the lifetime is generally longer than half the dephasing time, i.e., $T_1 \geq T_2/2$.

In order to clarify whether the observed thickness dependence of the biexciton dephasing time in Fig. 3 is an intrinsic phenomenon, we measured the exciton lifetime. Figure 4(a) shows the PP responses for $d = 6, 50$ nm samples when the center of the excitation laser spectrum was tuned to the exciton resonance at 3.202 eV. The PP signal in each scan shows a single exponential decay, which reflects the exciton population dynamics. The exciton lifetimes are estimated to be $T_1^E \sim 3.7$ ps for $d = 6$ nm and $T_1^E \sim 0.25$ ps for $d = 50$ nm by a single exponential fitting. Figure 4(b) shows the thickness dependences of the exciton lifetime T_1^E and $1/T_1^E$ with a thickness range of 6–100 nm. In CuCl crystals, the exciton

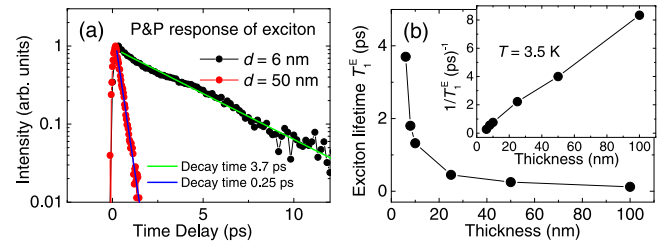


FIG. 4. (a) PP responses for the $d = 6$ and 25 nm samples, together with fitting curves, when the center of the excitation laser spectrum was in resonance with the exciton. (b) Thickness dependence of the exciton lifetime T_1^E . The inset shows the dependence of $1/T_1^E$ on the thickness.

Bohr radius is much smaller than our sample thicknesses. Therefore, the center-of-mass (c.m.) motion of the exciton wave function is affected solely by the sample thickness, and the c.m. wave function along the z axis parallel to the growth axis is quantized as $\propto \sin(n\pi z/d)/\sqrt{d}$, where n denotes a quantum number for satisfying a boundary condition at the sample surfaces. Recent studies on exciton systems [16–18] have demonstrated a change in the exciton-photon coupling energy of each exciton state dependent on thickness and have pointed out that the maximum coupling energy of the higher $n \geq 2$ states is larger than that of the lowest $n = 1$ exciton, depending on the thickness. The theoretical calculation with the assumption of an ideal condition for CuCl films has predicted that the largest value of $1/T_1^E$ of the exciton states was almost proportional to the thickness [17]. Our obtained dependence in the inset of Fig. 4(b) is consistent with that of the calculation. According to the theoretical calculation [17], the lowest $n = 1$ exciton gives maximum values of $1/T_1^E$ of $\sim 1, 3,$ and 5 ps^{-1} for thicknesses of $d = 10, 25,$ and 50 nm, respectively. For $d = 100$ nm, the $n = 2$ exciton yields a maximum $1/T_1^E$ of ~ 9 ps^{-1} . Therefore, the experimentally estimated $1/T_1^E$ at each thickness in the inset of Fig. 4(b) also agrees well quantitatively with the theoretically expected value, indicating that nonradiative processes arising from the crystal qualities and roughness of sample surfaces can be neglected within our measured timescale. In addition, the lack of correlation between the thickness dependences of the exciton lifetime and the biexciton dephasing time supports the assumption of a negligible contribution of a nonradiative relaxation process to the exciton and biexciton relaxation processes because the dominance of a nonradiative decay process would cause the same thickness dependences of the exciton and the biexciton.

Here, for the $d = 130$ and 200 nm samples, we could not extract the exciton lifetime within our simple exponential fitting for the following reason. At thicknesses larger than 100 nm, many higher exciton states with large coupling energy begin to contribute to the optical response [16–18], making the decay profiles of the PP signal sensitive to the probe wavelength (data not shown), as can be seen in a transient grating experiment with a high-quality CuCl film [18]. The contribution of the higher states requires a more advanced procedure, like that in Ref. [18], to estimate the exciton lifetime.

Next, we discuss the appearance of the fast decay component arising from the exciton in the TR-TPPS decay profiles for the $d \geq 100$ nm samples, as shown in Figs. 2(c) and 2(d), when the central photon energy of the excitation laser is in two-photon resonance with the biexciton. As described above, thicker samples give larger exciton-photon coupling energy. In addition, the exciton state with the lowest energy is shifted to the lower-energy side with increasing thickness, referred to as radiative shift [16–18]. Therefore, in the $d \geq 100$ nm samples, the lowest-energy exciton is partially covered with the excitation laser spectrum. The large exciton-photon coupling energy induces strong optical nonlinearities and contributes to the TR-TPPS signal as an additional signal, which reflects the fast population decay of the exciton. With increasing thickness, the lowest-energy exciton approaches the center of the laser spectrum. Therefore, the signal ratio between the exciton and the biexciton increases with the thickness, as can be seen in Figs. 2(c) and 2(d).

IV. THEORETICAL ANALYSIS

In confinement structures, there are four types of radiative relaxation processes of a biexciton. One is dissociation into a one-exciton-one-photon state, which corresponds to the biexciton spontaneously emitting a photon outside the crystal and the recoil exciton staying in the crystal. Another is the transition to a two-surface-polariton state, which represents a surface polariton pair. The others are one in which the biexciton decays to a one-exciton-one-surface-polariton state and a one-photon-one-surface-polariton state.

First, let us focus on the role of the surface polariton in the biexciton dissociation process. The surface polariton is one of the exciton-photon coupled states, which propagates along the in-plane direction of the sample with an in-plane wave vector k_{\parallel} . When we set the growth direction to the z axis and assume that the polariton propagates along the x axis, there are three modes, i.e., X -, Y -, and Z -mode surface polaritons. The mode depends on the polarization direction. The polarization of the X -mode is parallel to the propagating direction, which corresponds to a longitudinal wave. The Y -mode is a purely transverse wave and is polarized along the y axis. For the Z mode, the polarization is along the z axis. The dispersion relations of these polaritons have been theoretically calculated by semiclassical treatments [29–32], and only the exciton component in the wave function of the Y -mode surface polariton has been phenomenologically obtained [22]. Recently, one of the authors quantum mechanically derived both the exciton and photon components in the Y -mode surface polariton [33] using Fano's method [34], which gives an opportunity for analyzing the transition rate from the biexciton to the surface polariton pairs, typically, the Y -mode surface polariton.

Figure 5(a) shows the theoretically calculated thickness dependence of the dispersion curve for the lower Y -mode surface polariton for a CuCl film when the excitonic dipole moment is assumed to have the same value as a bulk crystal, which is obtained by the splitting energy between the longitudinal and transverse excitons, i.e., L - T splitting. For simplicity, in Fig. 5, we calculate the case of the lowest $n = 1$ exciton state. The c.m. wave function, written as $\propto \sin(n\pi z/d)/\sqrt{d}$, gives a thickness dependence $\propto \sqrt{d}$ to the exciton-photon coupling energy of the

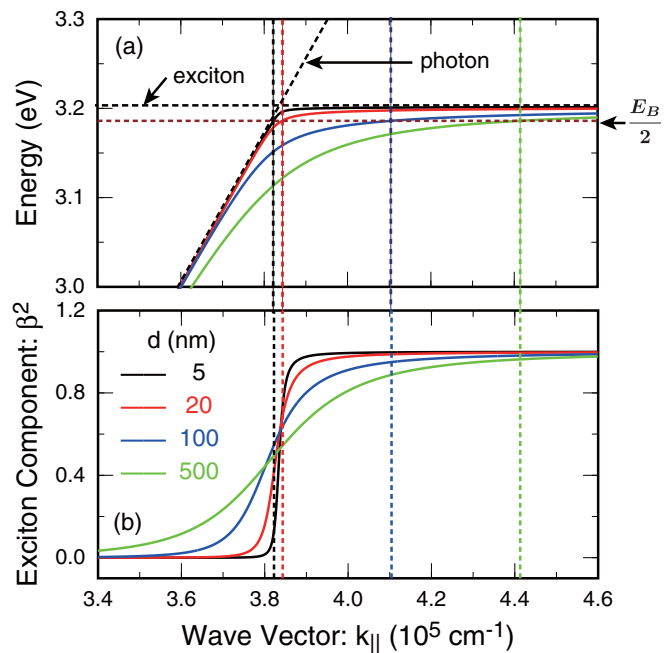


FIG. 5. (a) Calculated dispersion curves for the lower surface polariton with various thicknesses. (b) Calculated exciton component β^2 in the lower surface polariton as a function of the in-plane wave vector with various thicknesses. β denotes the probability amplitude of the exciton in the lower surface polariton.

surface polariton. Therefore, the splitting energy of the upper and lower polaritons depends on the sample thickness.

In our experiment using the pump pulse with an incident angle normal to the sample surface, we create a biexciton with an in-plane wave vector $k_{\parallel} = 0$. The surface polaritons dissociated from the biexciton satisfy the wave vector and energy conservation laws, i.e., $k_{1\parallel} + k_{2\parallel} = 0$ and $E_1 + E_2 = E_B$, respectively, where $k_{1,2\parallel}$ represent the in-plane wave vectors of the dissociated surface polaritons and $E_{1,2}$ are their energies. E_B denotes the biexciton energy. Therefore, each dissociated polariton has the same energy, $E_{sp} = E_B/2 = 3.186$ eV. At an intersection point between the energy $E_{sp} = 3.186$ eV and the dispersion curve of the surface polariton, we can find the wave vector of the dissociated polaritons, which varies the exciton-photon composition in the dissociated polariton in Fig. 5(b). On the other hand, the transition moment from the biexciton $|B\rangle$ to the two-polariton state $|P_{k_{\parallel}}, P_{-k_{\parallel}}\rangle$ with the in-plane wave vectors opposite each other is written as $|\langle P_{k_{\parallel}}, P_{-k_{\parallel}} | H_{ep} | B \rangle|^2$, where H_{ep} represents the interaction Hamiltonian, which describes the transition between the biexciton state and the one-exciton-one-photon state. Therefore, the transition moment is affected by the thickness through a variation in the exciton-photon composition in the surface polariton, which exhibits anomalous dependence on the thickness of the crystal.

In order to confirm that the above relaxation process is a dominant process, we calculated the dissociation time (lifetime) of the biexciton for the four dissociation processes as a reciprocal of the transition rate, which is a product of the transition moment and the density of the final states. Figure 6 shows the results. We used the same values of the physical

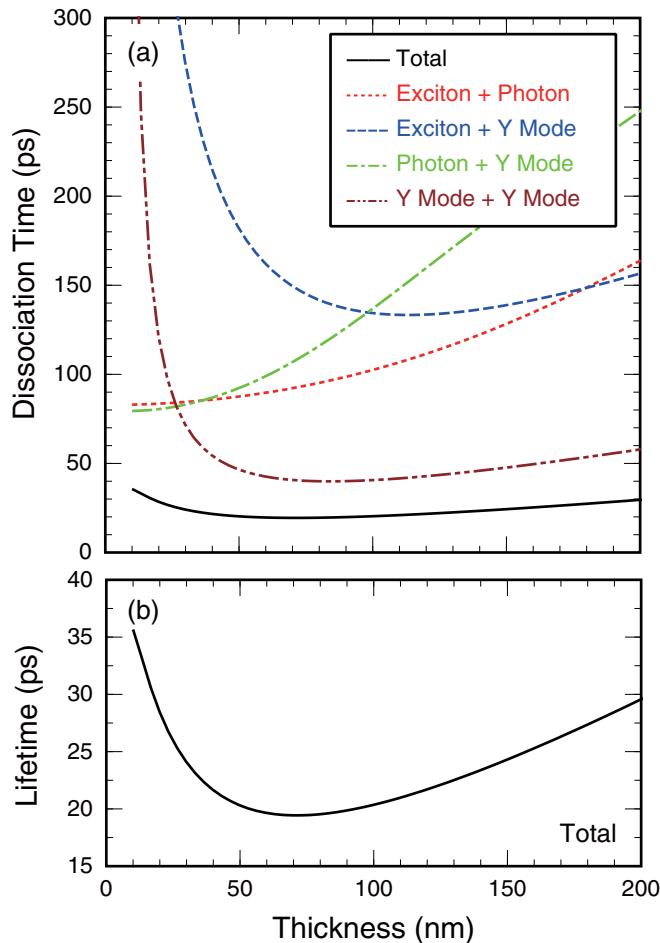


FIG. 6. (a) Calculated thickness dependences of the biexciton dissociation time in the one-exciton-one-photon state (labeled Exciton + Photon), the Y -mode surface polariton pair state (Y Mode + Y Mode), one-photon-one- Y -mode-surface-polariton state (Photon + Y Mode), and one-exciton-one- Y -mode-surface-polariton state (Exciton + Y Mode), together with the total dissociation time. (b) Calculated biexciton lifetime (total dissociation time) as a function of the thickness

parameters for the exciton as in Fig. 5. The biexciton wave function was obtained with a tight-binding model [35]. As seen in Fig. 6(a), the dissociation into the surface polariton pair dominates the biexciton lifetime in the regime thicker than $d \sim 20$ nm, while for the thinner regime, the dissociation into the one-exciton-one-photon state and the one-photon-one- Y -mode-surface-polariton state governs the lifetime. As shown in Fig. 6(b), the calculated curve for the total dissociation time (lifetime) is downward convex, very similar to the experimental data in Fig. 3. This characteristic feature mainly arises from

the dissociation process into the surface polariton pair. The shortest dissociation time is realized at the thickness giving the maximum transition moment when the dissociated polaritons contain the photon and exciton components equally.

In Fig. 6(b), the minimum lifetime appears at a greater thickness than the observation, and the calculated lifetime is an order of magnitude longer. The quantitative difference arises from the lack of final states in the calculation because we took into account only the Y -mode surface polariton. In addition, the higher $n \geq 2$ exciton states were not considered. As mentioned before, depending on the thickness, the maximum exciton-photon coupling energy of the higher states is larger than that of the lowest exciton [16–18]. The higher states with larger exciton-photon coupling energy give rise to a shorter dissociation time and enlarge the splitting energy around the anticrossing point in the dispersion relation, indicating that the thickness giving the minimum lifetime moves to the thinner regime. Therefore, we expect that the calculations will more suitably reproduce the observations by introducing the other surface polariton modes and the change in the coupling energy due to the thickness. Nevertheless, the qualitative agreement with the observed and calculated dependences indicates that the biexciton relaxation process is dominated by the dissociation into the surface polariton pair in the measured thickness regime.

Finally, our results show that the biexciton in a thin film can be efficiently converted into a surface polariton pair by controlling the film thickness. We expect that the surface polariton pair can be easily extracted as a photon pair from the film by a standard method using a prism [36,37], which leads to the possibility of a novel scheme for high-efficiency photon pair generation without a cavity.

V. CONCLUSION

In conclusion, we observed the unique thickness dependence of the biexciton relaxation time in CuCl films, while the exciton lifetime showed monotonic dependence on the thickness. We calculated the biexciton relaxation time with the assumption of the simple relaxation processes. The qualitative agreement between the thickness dependences of the observation and the calculation shows that the surface polariton is essential to the biexciton relaxation process in the measured thickness regime.

ACKNOWLEDGMENTS

We would like to thank M. Sadgrove of Tohoku University for helpful discussions. We are also grateful to M. Ueda of Osaka City University for his help with the sample preparation. This work was supported by JSPS KAKENHI Grants No. JP16K05403, No. JP15H03678, No. JP22244035, and No. JP24654081.

- [1] E. Hanamura, *Solid State Commun.* **12**, 951 (1973).
- [2] G. M. Gale and A. Mysyrowicz, *Phys. Rev. Lett.* **32**, 727 (1974).
- [3] N. Nagasawa, N. Nakata, Y. Doi, and M. Ueta, *J. Phys. Soc. Jpn.* **39**, 987 (1975).
- [4] T. Itoh and T. Suzuki, *J. Phys. Soc. Jpn.* **45**, 1939 (1978).

- [5] M. Ueta, T. Mita, and T. Itoh, *Solid State Commun.* **32**, 43 (1979).
- [6] R. Shimano and M. Kuwata-Gonokami, *Phys. Rev. Lett.* **72**, 530 (1994).
- [7] K. Edamatsu, G. Oohata, R. Shimizu, and T. Itoh, *Nature (London)* **431**, 167 (2004).

- [8] G. Oohata, R. Shimizu, and K. Edamatsu, *Phys. Rev. Lett.* **98**, 140503 (2007).
- [9] C. L. Salter, R. M. Stevenson, I. Farrer, C. A. Nicoll, D. A. Ritchie, and A. J. Shields, *Nature (London)* **465**, 594 (2010).
- [10] H. Akiyama, M. Kuwata, T. Kuga, and M. Matsuoka, *Phys. Rev. B* **39**, 12973 (1989).
- [11] H. Akiyama, T. Kuga, M. Matsuoka, and M. Kuwata-Gonokami, *Phys. Rev. B* **42**, 5621 (1990).
- [12] T. Ikehara and T. Itoh, *Solid State Commun.* **79**, 755 (1991).
- [13] K. Kurihara, E. Tokunaga, M. Baba, and M. Matsuoka, *Phys. Rev. B* **52**, 8179 (1995).
- [14] E. Vanagas, J. Kudrna, D. Brinkmann, P. Gilliot, and B. Hönerlage, *Phys. Rev. B* **63**, 153201 (2001).
- [15] M. Nakayama, S. Wakaiki, K. Mizoguchi, D. Kim, H. Ichida, and Y. Kanematsu, *Phys. Status Solidi C* **3**, 3464 (2006).
- [16] M. Ichimiya, M. Ashida, H. Yasuda, H. Ishihara, and T. Itoh, *Phys. Status Solidi B* **243**, 3800 (2006).
- [17] M. Bamba and H. Ishihara, *Phys. Rev. B* **80**, 125319 (2009).
- [18] M. Ichimiya, M. Ashida, H. Yasuda, H. Ishihara, and T. Itoh, *Phys. Rev. Lett.* **103**, 257401 (2009).
- [19] Y. Masumoto, Y. Unuma, Y. Tanaka, and S. Shionoya, *J. Phys. Soc. Jpn.* **47**, 1844 (1979).
- [20] Y. Masumoto and S. Shionoya, *J. Phys. Soc. Jpn.* **51**, 181 (1982).
- [21] T. Ikehara and T. Itoh, *Phys. Rev. B* **44**, 9283 (1991).
- [22] A. L. Ivanov, H. Wang, J. Shah, T. C. Damen, L. V. Keldysh, H. Haug, and L. N. Pfeiffer, *Phys. Rev. B* **56**, 3941 (1997).
- [23] M. Nakayama, T. Nishioka, S. Wakaiki, G. Oohata, K. Mizoguchi, D. Kim, and K. Edamatsu, *Jpn. J. Appl. Phys.* **46**, L234 (2007).
- [24] K. B. Ferrio and D. G. Steel, *Phys. Rev. B* **54**, R5231(R) (1996).
- [25] W. Langbein and J. M. Hvam, *Phys. Rev. B* **61**, 1692 (2000).
- [26] Y. Mitsumori, S. Matsuura, S. Uchiyama, K. Edamatsu, and M. Nakayama, *Phys. Rev. B* **94**, 115308 (2016).
- [27] T. Yajima and Y. Taira, *J. Phys. Soc. Jpn.* **47**, 1620 (1979).
- [28] D. K. Shuh, R. S. Williams, Y. Segawa, J.-i. Kusano, Y. Aoyagi, and S. Namba, *Phys. Rev. B* **44**, 5827 (1991).
- [29] M. Nakayama, *Solid State Commun.* **55**, 1053 (1985).
- [30] M. Nakayama and M. Matsuura, *Surf. Sci.* **170**, 641 (1986).
- [31] F. Tassone, F. Bassani, and L. C. Andreani, *Nuovo Cimento D* **12**, 1673 (1990).
- [32] F. Tassone, F. Bassani, and L. C. Andreani, *Phys. Rev. B* **45**, 6023 (1992).
- [33] H. Ajiki, *Phys. Rev. B* **92**, 155316 (2015).
- [34] U. Fano, *Phys. Rev.* **124**, 1866 (1961).
- [35] H. Ajiki, *J. Chem. Phys.* **142**, 104110 (2015).
- [36] F. Yang, J. R. Sambles, and G. W. Bradberry, *Phys. Rev. Lett.* **64**, 559 (1990).
- [37] F. Yang, J. R. Sambles, and G. W. Bradberry, *Phys. Rev. B* **44**, 5855 (1991).